Nanoscale

RSC Publishing

COMMUNICATION

View Article Online
View Journal | View Issue

Cite this: *Nanoscale*, 2013, **5**, 5715

Received 13th March 2013
Accepted 29th April 2013

DOI: 10.1039/c3nr01284k

www.rsc.org/nanoscale

Measurements of contact specific low-bias negative differential resistance of single metalorganic molecular junctions†

Jianfeng Zhou,[a] Satyabrata Samanta,[b] Cunlan Guo,[a] Jason Locklin[b] and Bingqian Xu*[a]

Negative differential resistance (NDR) behaviors of single molecule junctions composed of a thiol-terminated Ru(II) bis-terpyridine ($Ru(tpy\text{-}SH)_2$) molecule sandwiched between two gold electrodes are measured using a specifically modified scanning probe microscope break junction technique (SPMBJ) at room temperature. The low-bias (0.623 ± 0.135 V) NDR observed for one of the three conductance groups is contact specific and is caused by a bias induced electrode–molecule coupling changes.

In the field of molecular electronics, molecular junctions have attracted significant attention in the past decade due to their potential for device applications at the single molecule level.[1,2] Many interesting physical properties, such as conductance, ratifications, negative differential resistance (NDR), switching and amplifications, have been demonstrated in molecular junctions based on single molecules.[3–5] The NDR effect, which is described by a decreasing current through the junction with an increasing bias voltage, has been observed in various systems and was believed to be significant to construct molecular switches and molecular transistors for future device applications.[4,6–10] Alongside the experimental observations, theoretical studies have proposed various mechanisms to reveal the origin of NDR, which can be roughly grouped into molecular core focused and molecule–electrode focused mechanisms. For the molecule–core focused mechanism, the NDR phenomena were attributed to charge blocking caused by bias induced redox reactions.[11–15] Some groups[16–18] have also suggested that NDR behavior was mainly caused by the conformation changes of the molecular core induced by external bias.[11,14,19] In a junction with weakly coupled contacts, researchers have stated that the narrow density of state (DOS) features of the tip apex of electrodes contribute to the observed NDR behavior.[20–22] In contrast, for the molecular junctions with strongly coupled contacts,[23–25] the molecule and the electrodes need to be studied as a whole, although most of the studies have not elaborated on the bias-induced molecule–electrode coupling.[24] To unravel the true mechanism of NDR in a strongly coupled molecule junction experimentally, the single molecular junction properties must be studied in detail with more controllable techniques. To the best of our knowledge, no such measurement has been reported in the literature.

Herein we report our measurement of controlled electronic transport in single molecule junctions composed of a thiol-terminated Ru(II) bis-terpyridine ($Ru(tpy\text{-}SH)_2$) molecule sandwiched between two gold electrodes using a specifically modified scanning probe microscope break junction technique (SPMBJ).[26,27] We chose $Ru(tpy\text{-}SH)_2$ in this study due to the promising conductivities and optical excitation properties that have been observed in the literature,[28,29] and particularly because of a theoretically predicted NDR for metal–terpyridine molecular junctions.[24] We believe the conclusions drawn based on the single molecular behavior of metal–terpyridine molecular junctions will be helpful in explaining the formation mechanisms of nonlinear behavior observed in a series of metal–organic molecular junctions.[30–35] $Ru(tpy\text{-}SH)_2$ was synthesized by following the procedure described in the ESI (SI-1†). Gold substrates and SPM tips were prepared according to the procedures described in our previous publications.[26,27] Two different solution experiments were performed in order to investigate the influence of metal ions on the conductance behavior in the molecular junctions. A solution containing either 1 mM of the tpy-SH ligand or the $Ru(tpy\text{-}SH)_2$ complex was prepared in tetrahydrofuran (THF) solution and put into SPM liquid cells on separate gold substrates. After immersion in static solution for 6 hours, the molecules form Self-Assembled Monolayers (SAMs) on the substrates (SI-2†) and were used in the next step for SPMBJ measurements in the solution.

[a]*Single Molecule Study Laboratory, College of Engineering and Nanoscale Science and Engineering Center, University of Georgia, Athens, GA 30602, USA. E-mail: bxu@engr.uga.edu; Fax: +1-706-542-3804; Tel: +1-706-542-0502*

[b]*Complex Carbohydrate Research Center and Department of Biochemistry and Molecular Biology, University of Georgia, Athens, GA 30602, USA*

† Electronic supplementary information (ESI) available. See DOI: 10.1039/c3nr01284k

SPMBJs[36,37] have been widely used in measuring electronic transport properties in single molecular junctions. However the measured conductance complicates the interpretations due to the continuous modification of the contact configurations introduced by the continuous retraction of the SPM tip. The fundamental concept of this new approach is to fabricate stabilized single molecule junctions to minimize the contact conformation complexities. As illustrated in Fig. 1, single molecule junctions (Fig. 1(a)) were produced by dividing the continuous retraction into two processes: an abrupt stretching and free holding (Fig. 1(c), black curve) to keep the junctions at specific contact configurations.[26,27] Single molecule conductance determined by the conductance histograms (Fig. 1(b)) was used to determine the current value of the stabilized molecule junctions (Fig. 1(c)). We then introduced bias sweeping during which the Ru(tpy-SH)$_2$ molecule was freely held between Au electrodes (Fig. 1(a) and (c)). In this way, *I–V* characteristic behavior of single Ru(tpy-SH)$_2$ molecular junctions (Fig. 1(d)) can be reproduced during the formation of the molecular junctions. To make certain that during the bias sweep the junction is stabilized and contains only a single Ru(tpy-SH)$_2$ molecule, we produced stabilized molecular junctions at a bias of 0.3 V (a and b in Fig. 1(c)) and chose a smaller region of the sweep (c and d in Fig. 1(c)) so as to check the same conductance before (c′ in Fig. 1(c)) and after (d′ in Fig. 1(c)) the bias sweep at 0.3 V for all experiments (Fig. 1(c)). The bias-sweep range in our experiments was always −1.0 V to 1.0 V.

To determine the conductance of Ru(tpy-SH)$_2$ molecule junctions, we applied the modified SPMBJ method and used the stretching–holding approach. The results demonstrated three conductance sets with single molecular conductance values $G_L = 3.1 \times 10^{-5} G_0$ (low), $G_M = 4.3 \times 10^{-5} G_0$ (medium), and $G_H = 1.13 \times 10^{-5} G_0$ (high), respectively (Fig. 1(b) and SI-3†). The multiple single molecular conductance sets have also been reported for other types of molecular junctions.[12,27,38,39] Different single molecular conductance sets should correspond to different contacts formed in molecular junctions.[40–42] Thus, we believe the different single molecular conductance values observed here can also be attributed to the different preferential contact conformations in the stable Ru(tpy-SH)$_2$ molecular junctions.[24,43,44] More specifically, the 3 conductance sets have been related to the binding configurations of the molecule–electrode interface[45,46] and accordingly our measured conductance G_H should correspond to the hollow–hollow configuration, G_M the hollow–top configuration, and G_L the top–top configuration. In addition, as is shown in previous reports,[47] the estimated single molecular conductance of Co–terpyridine molecular junctions measured for junctions consisting of multiple molecules ranges from $0.8 \times 10^{-6} G_0$ to $0.75 \times 10^{-4} G_0$, close to our measured conductance for single Ru(tpy-SH)$_2$ molecule junctions. However, because of the added controls, we believe our experimental results provide more precise single conductance features of metal–terpyridine molecular junctions than previously reported ones.

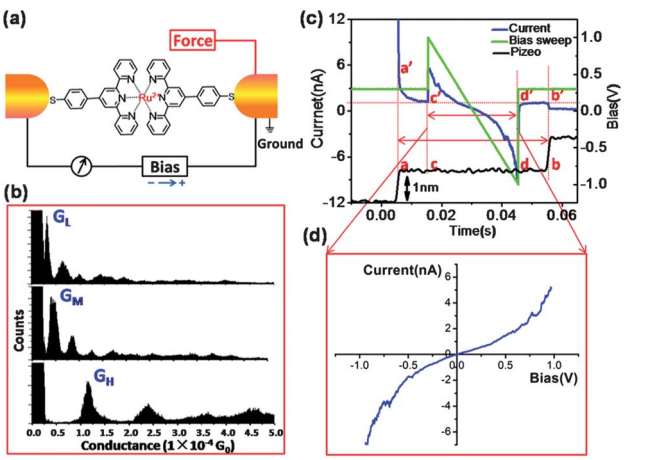

Fig. 1 (a) Schematic diagram of the Ru(tpy-SH)$_2$ molecular junction. (b) Conductance histograms of Ru(tpy-SH)$_2$ molecular junctions, resolved three conductance sets with single molecular conductance values (G_L, G_M, and G_H). (c) A typical curve for G_L with bias sweeping during the free holding process. c′ and d′ are used to label the conductance plateau at the start and end of the bias sweep to make sure that a single molecule was wired in the measured molecular junctions. (d) The *I–V* curve converted from (c) with current (blue) *versus* bias (green).

Compared to static conductance results at a certain bias, *I–V* characteristic curves of single molecular junctions can provide more information about electron transport properties of target molecules. Using the techniques described in Fig. 1, we measured the *I–V* curves of both the tpy-SH ligand molecular junctions and the Ru(tpy-SH)$_2$ molecule junctions of all the three conductance sets (Fig. 2). Firstly, we found that the Ru(tpy-SH)$_2$ molecule junctions have a much larger single molecular conductance (G_L, G_M, and G_H, see Fig. SI-2†) than that for the tpy-SH ligand molecular junctions (G_N) (Fig. 2(a)). The ratio of the conductance of G_M and G_N(G_M/G_N) ranges from about 50 to 250 at different bias (Fig. 2(b)), which agrees with the previous experimental[48,49] and theoretical studies.[32] Remarkably, for Ru(tpy-SH)$_2$ molecule junctions, more than 20% of the *I–V* characteristic curves (55/233 curves) are found to belong to the set of G_M that show obvious negative differential resistance (NDR) behaviors (labeled red) while the curves in other two single molecular conductance sets (G_L and G_H) do not show similar phenomena. These results clearly suggested that the NDR effect observed in our experiments is not only intrinsic to Ru(tpy-SH)$_2$ but also contact conformation dependent.

To demonstrate that NDR is intrinsic to Ru(tpy-SH)$_2$, we compared the *I–V* curves of very well studied octanedithiol (C8DT) molecular junctions using the same methods (Fig. SI-4†). We found that the *I–V* curves of Ru(tpy-SH)$_2$ molecular junctions show more nonlinear behavior when at bias voltage greater than about 0.4 V. To explain this phenomenon, we constructed the numerical differential conductance profiles (d*I*/d*V* *versus* *V*) of Ru(tpy-SH)$_2$ and C8DT molecular junctions. The differential conductance profiles were used to interpret the local density of state (LDOS) of whole molecular junctions in the bias sweeping ranges.[50–52] With a −1.0 to +1.0 V bias sweeping range, Fig. 3 shows some LDOS peaks in the differential conductance profile of Ru(tpy-SH)$_2$ while for C8DT, the profile is relatively smooth. We believe those peaks involved in LDOS should be responsible for the observed nonlinear behavior[53] of Ru(tpy-SH)$_2$ molecular junctions. Furthermore, as is known, the

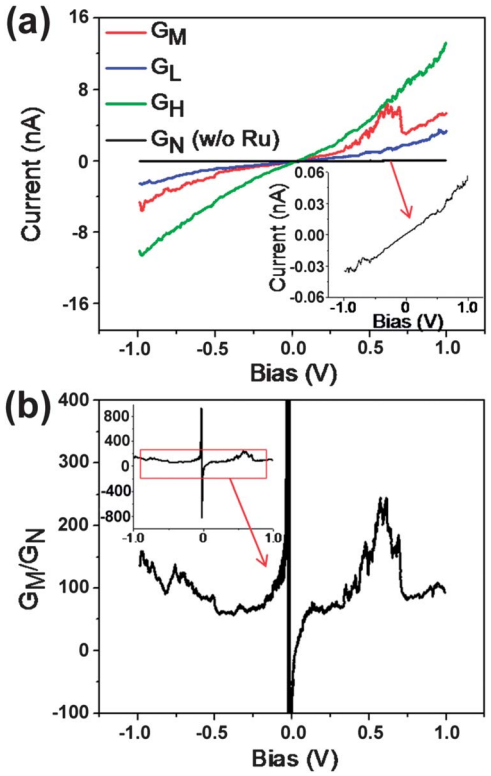

Fig. 2 (a) *I–V* curves for Ru(tpy-SH)$_2$ molecule junctions without a Ru-ion center (G_N: black) and for the junctions with a Ru-ion center of three sets of conductance (G_L: green, G_M: red, and G_H: blue). Inset: zoom-in of the *I–V* curve for G_N. (b) Current ratio of G_M to G_N (G_M/G_N) *vs.* bias voltage plot, showing that G_M is 50 to 250 times that of G_N.

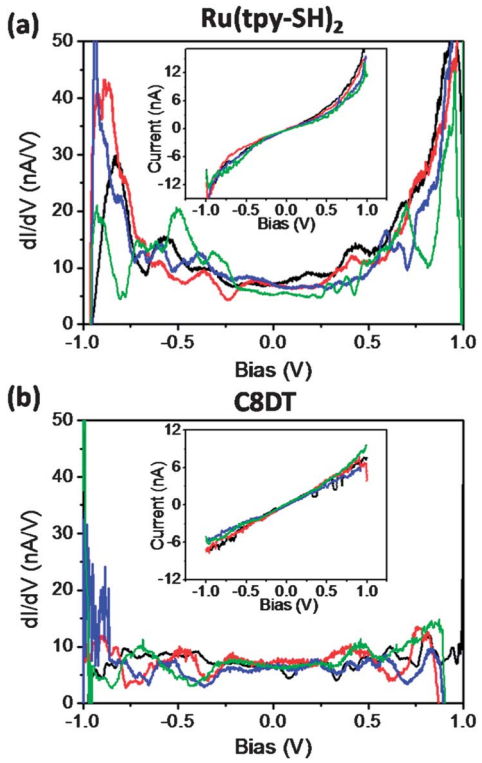

Fig. 3 Numerical differential conductance curves (d*I*/d*V versus* bias *V*) for (a) Ru(tpy-SH)$_2$ and (b) C8DT. The insets in (a) and (b) are the *I–V* curves used to construct d*I*/d*V* for Ru(tpy-SH)$_2$ and C8DT, respectively. As an example, the conductance $G_H = 1.13 \times 10^{-4}G_0$ for Ru(tpy-SH)$_2$ and $G_{S3} = 0.9 \times 10^{-4}G_0$ for C8DT was compared. Other conductance sets of each molecule show similar behaviors.

current would continue to increase linearly with increasing bias because the bias sweeping is much smaller than the HOMO–LUMO gap of the molecular core.[54] In contrast, for molecular junctions with smaller HOMO–LUMO gaps, at room temperature, the density of states distribution should be relatively broadened. Partial state density distributions may be involved in the bias sweeping range, which are responsible for the extra peaks observed in Fig. 3(a) and lead to nonlinear behavior at higher bias. Thus, the smaller HOMO–LUMO gap (3–4 eV) of Ru(tpy-SH)$_2$ (ref. 33) compared to that of C8DT (10 eV energy gap) should be considered as a main reason for the nonlinear behavior observed in Ru(tpy-SH)$_2$ molecular junctions.[55] In addition, the hybridization among the transition metal center, organic molecule backbone and Au electrodes would possibly cause a complex energy profile or even introduce some extra steady-states. It might also contribute to the nonlinear behavior at higher bias for Ru(tpy-SH)$_2$ molecular junctions.

Besides Ru(tpy-SH)$_2$ molecular cores, NDR behaviors in our system are only observed for one (G_M) of the three conductance sets, which is related to a specific contact conformation. It is often assumed that the contact conformations have a significant impact on the electron transport through molecular junctions.[56–58]

In the strongly coupled system, Pati *et al.* have recently proposed a unified model which attributed the NDR effect to the nonlinear changes in the coupling between the molecule and lead induced by external bias.[24] However, in their report, the NDR peak appears at a bias of about 3.4 V, much higher than our observed 0.623 ± 0.135 V bias voltage (Fig. 4(a)). For the low bias NDR behavior induced by strong coupling in the contacts, a recent study proposed that it should be attributed to the specific contact conformations,[59] which is supported by our experimental results. Specifically, Pati *et al.* further reported in their most recent paper[60] that current switches on only for the hollow–top junction contact conformation.

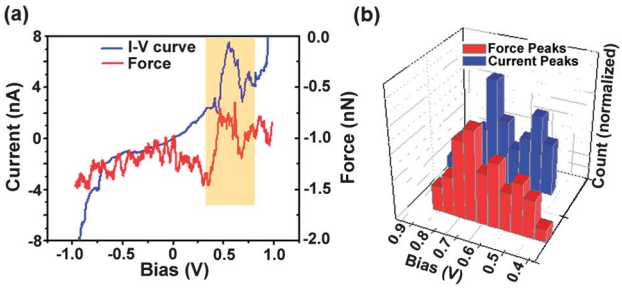

Fig. 4 (a) Representative monitored *I–V* curves (blue) and force changes (red) with bias sweeping. The shaded area highlights the NDR and force peaks. (b) The histograms of the NDR peak position (blue) and force peak position (red) using 50 curves each as shown in (a). Statistically, the NDR peaks are located at 0.623 ± 0.135 V while the force peaks are located at a bias of 0.601 ± 0.171 V.

To prove that the observed NDR for the specific contact conformation (conductance of G_M) is also the result of bias induced coupling changes, we simultaneously monitored the force changes during the bias sweep. Fig. 4(a) shows a typical *I–V* curve and the corresponding force curve demonstrating that the greatest change in force happens at the bias where NDR is observed. For both the individual curves and statistical results using 50 curves, the NDR peak always accompanies a force peak (Fig. 4). The peaks of average force changes are located at a bias of 0.601 ± 0.171 V (Fig. 4(b)) and a value for force changes of 0.319 ± 0.098 nN was observed. The force changes agree with our earlier measurements of electrode interfaces of single molecule junctions by controllable mechanical modulations[61–63] and thus it is likely caused by molecule–electrode coupling changes induced by the bias. It is also possible that conformational relaxation of molecular junctions could be caused by a bias induced twist of molecular structures or bias charging on a redox active center as a polaron model.[16–18] However, the underlying mechanisms of conformation changes in our system under specific bias conditions still need further systematic studies, specifically with respect to theoretical calculations. Besides, the NDR was only observed at the positive bias and this *I–V* asymmetry could be caused by the asymmetric channel coupling upon the applied bias, even for symmetric junctions.[24] The exact reason, however, deserves further theoretical simulations to be determined.

The NDR behavior in our system was observed at low bias at room temperature. As an important parameter, the peak-to-valley current ratio (PVR) is always used to describe the degree of NDR. In our studies, PVR can be directly obtained by comparing the peak current to the valley current in the *I–V* curves. The average PVR from statistical results is 1.47 ± 0.21 : 1. This PVR value is small, which is common at room temperature. In Chen's report,[6] a PVR of around 1000 : 1 at low temperature only showed 1.5 : 1 PVR at room temperature. The degradation of NDR behavior is believed to be due to the increased inelastic scattering at higher temperature. This explanation also agrees with our proposed mechanism. Possible improvements to achieve more satisfactory PVRs in the future could be expected by controlling the conformation variation process and reducing inelastic scattering with confined freedom of thermal fluctuations.

In summary, we have applied a specially modified SPMBJ to characterize electronic transport properties of Ru(tpy-SH)$_2$ molecular junctions. For the first time, we have directly measured the electron transport properties of Ru(tpy-SH)$_2$ molecular junctions at the single molecular level. We found that the existence of a bridging Ru(II) ion increases the conductance of molecular junctions by at least 2 orders of magnitudes with respect to the ligand alone. Three different single molecular conductance sets due to different contact conformations were identified, and single molecular *I–V* characteristic curves for the three different contact conformations were measured by performing the bias sweep for stabilized junctions. The *I–V* curves of Ru(tpy-SH)$_2$ molecular junctions show nonlinear behavior at relatively higher bias compared to the C8DT molecular junctions due to specific electronic properties of Ru(tpy-SH)$_2$ molecules. NDR behaviors were also observed in the single molecular *I–V* curves related to a specific contact conformation. By comparing with the simultaneous force signal, we directly proved that the coupling between the Ru(tpy-SH)$_2$ molecular core and contacts results in observed NDR behavior. Although further experimental and theoretical efforts will still be needed to test and complete our proposed mechanisms in the future, our results provide a possible mechanism to explain nonlinear behaviors, particularly the NDR effect, in other metal–organic complex molecules.

Acknowledgements

This work is supported by the U.S. National Science Foundation: ECCS 0823849 and ECCS 1231967 (B.X.).

References

1 S. W. Herwald and S. J. Angello, *Science*, 1960, **132**, 1127–1133.
2 C. Joachim and M. A. Ratner, *Proc. Natl. Acad. Sci. U. S. A.*, 2005, **102**, 8801–8808.
3 A. Aviram and M. A. Ratner, *Chem. Phys. Lett.*, 1974, **29**, 277–283.
4 J. Chen, M. A. Reed, A. M. Rawlett and J. M. Tour, *Science*, 1999, **286**, 1550–1552.
5 N. J. Tao, *Nat. Nanotechnol.*, 2006, **1**, 173–181.
6 J. Chen, W. Wang, M. A. Reed, A. M. Rawlett, D. W. Price and J. M. Tour, *Appl. Phys. Lett.*, 2000, **77**, 1224–1226.
7 I. Kratochvilova, M. Kocirik, A. Zambova, J. Mbindyo, T. E. Mallouk and T. S. Mayer, *J. Mater. Chem.*, 2002, **12**, 2927–2930.
8 J. D. Le, Y. He, T. R. Hoye, C. C. Mead and R. A. Kiehl, *Appl. Phys. Lett.*, 2003, **83**, 5518–5520.
9 A. M. Rawlett, T. J. Hopson, I. Amlani, R. Zhang, J. Tresek, L. A. Nagahara, R. K. Tsui and H. Goronkin, *Nanotechnology*, 2003, **14**, 377–384.
10 A. M. Rawlett, T. J. Hopson, L. A. Nagahara, R. K. Tsui, G. K. Ramachandran and S. M. Lindsay, *Appl. Phys. Lett.*, 2002, **81**, 3043–3045.
11 J. Cornil, Y. Karzazi and J. L. Brédas, *J. Am. Chem. Soc.*, 2002, **124**, 3516–3517.
12 Z. J. Donhauser, B. A. Mantooth, K. F. Kelly, L. A. Bumm, J. D. Monnell, J. J. Stapleton, D. W. Price, A. M. Rawlett Jr, D. L. Allara, J. M. Tour and P. S. Weiss, *Science*, 2001, **292**, 2303–2307.
13 J. M. Seminario, A. G. Zacarias and J. M. Tour, *J. Am. Chem. Soc.*, 2000, **122**, 3015–3020.
14 J. Taylor, M. Brandbyge and K. Stokbro, *Phys. Rev. B: Condens. Matter Mater. Phys.*, 2003, **68**, 121101(121101)–121101(121104).
15 M. D. Ventra, S.-G. Kim, S. T. Pantelides and N. D. Lang, *Phys. Rev. Lett.*, 2001, **83**, 288–291.
16 M. Galperin, M. A. Ratner and A. Nitzan, *Nano Lett.*, 2005, **5**, 125–130.
17 S. Yeganeh, M. Galperin and M. A. Ratner, *J. Am. Chem. Soc.*, 2007, **129**, 13313–13320.

18 A. Zazunov, D. Feinberg and T. Martin, *Phys. Rev. B: Condens. Matter Mater. Phys.*, 2006, **73**, 115405.
19 J. M. Seminario, P. A. Derosa and J. L. Bastos, *J. Am. Chem. Soc.*, 2002, **124**, 10266–10267.
20 M. Grobis, A. Wachowiak, R. Yamachika and M. F. Crommie, *Appl. Phys. Lett.*, 2005, **86**, 204102/1–204102/3.
21 B. Larade, J. Taylor, H. Mehrez and H. Guo, *Phys. Rev. B: Condens. Matter Mater. Phys.*, 2001, **64**, 075420/1–075420/10.
22 I. W. Lyo and P. Avouris, *Science*, 1989, **245**, 1369–1371.
23 M. Galperin, M. A. Ratner, A. Nitzan and A. Troisi, *Science*, 2008, **319**, 1056–1060.
24 R. Pati, M. McClain and A. Bandyopadhyay, *Phys. Rev. Lett.*, 2008, **100**, 246801(246801)–246801(246804).
25 X. Shi, X. Zheng, Z. Dai, Y. Wang and Z. Zeng, *J. Phys. Chem. B*, 2005, **109**, 3334–3339.
26 F. Chen, J. Zhou, G. Chen and B. Xu, *IEEE Sens. J.*, 2010, **10**, 485–491.
27 J. Zhou, F. Chen and B. Xu, *J. Am. Chem. Soc.*, 2009, **131**, 10439–10446.
28 L. Cai, M. A. Cabassi, H. Yoon, O. M. Cabarcos, C. L. McGuiness, A. K. Flatt, D. L. Allara, J. M. Tour and T. S. Mayer, *Nano Lett.*, 2005, **5**, 2365–2372.
29 J. P. Sauvage, J. P. Collin, J. C. Chambron, S. Guillerez, C. Coudret, V. Balzani, F. Barigelletti, L. D. Cola and L. Flamigni, *Chem. Rev.*, 1994, **94**, 4.
30 L. Chen, Z. Hu, A. Zhao, B. Wang, Y. Luo, J. Yang and J. G. Hou, *Phys. Rev. Lett.*, 2007, **99**, 146803(146801)–146803(146804).
31 A. K. Mahapatro, J. Ying, T. Ren and D. B. Janes, *Nano Lett.*, 2008, **8**, 2131–2136.
32 T. M. Perrine and B. D. Dunietz, *J. Phys. Chem. A*, 2008, **112**, 2043–2048.
33 K. Seo, A. V. Konchenko, J. Lee, G. S. Bang and H. Lee, *J. Am. Chem. Soc.*, 2008, **130**, 2553–2559.
34 E. Tran, C. Grave, G. M. Whitesides and M. A. Rampi, *Electrochem. Acta*, 2005, **50**, 4850–4856.
35 E. Tran, M. A. Rampi and G. M. Whitesides, *Angew. Chem., Int. Ed.*, 2004, **43**, 3835–3839.
36 B. Xu, X. Xiao and N. Tao, *J. Am. Chem. Soc.*, 2003, **125**, 16164–16165.
37 B. Xu and N. Tao, *Science*, 2003, **301**, 1221–1223.
38 F. Chen, C. Nuckolls and S. M. Lindsay, *Chem. Phys.*, 2006, **324**, 236–243.
39 X. Li, J. He, J. Hihath, B. Xu, S. M. Lindsay and N. J. Tao, *J. Am. Chem. Soc.*, 2006, **128**, 2135–2141.
40 K.-H. Müller, *Phys. Rev. B: Condens. Matter Mater. Phys.*, 2006, **73**, 045403(045401)–045403(045406).
41 A. Nishikawa, J. Tobita, Y. Kato, S. Fujii, M. Suzuki and M. Fujihira, *Nanotechnology*, 2007, **18**, 424005(424001)–424005(424010).
42 J. Tobita, Y. Kato and M. Fujihira, *Ultramicroscopy*, 2008, **108**, 1040–1044.
43 S. Piccinin, A. Selloni, S. Scandolo, R. Car and G. Scoles, *J. Chem. Phys.*, 2003, **119**, 6729–6735.
44 J. Tomfohr and O. F. Sankey, *J. Chem. Phys.*, 2004, **120**, 1542–1554.
45 F. Demir and G. Kirczenow, *J. Chem. Phys.*, 2011, **134**, 014703/1–014703/12.
46 C. M. Kim and J. Bechhoefer, *J. Chem. Phys.*, 2013, **138**, 014707/1–014707/6.
47 J. Tang, Y. Wang, J. E. Klare, G. S. Tulevski, S. J. Wind and C. Nuckolls, *Angew. Chem., Int. Ed.*, 2007, **46**, 3892–3895.
48 K. Liu, X. Wang and F. Wang, *ACS Nano*, 2008, **2**, 2315–2323.
49 J. Tang, Y. Wang, C. Nuckolls and S. J. Wind, *J. Vac. Sci. Technol., B: Microelectron. Nanometer Struct.–Process., Meas., Phenom.*, 2006, **24**, 3227–3229.
50 M. Elbing, R. Ochs, M. Koentopp, M. Fischer, C. v. Hänisch, F. Weigend, F. Evers, H. B. Weber and M. Mayor, *Proc. Natl. Acad. Sci. U. S. A.*, 2005, **102**, 8815–8820.
51 J. G. Kushmerick, D. B. Holt, J. C. Yang, J. Naciri, M. H. Moore and R. Shashidhar, *Phys. Rev. Lett.*, 2002, **89**, 086802(086801)–086802(086804).
52 Y. Noguchi, R. Ueda, T. Kubota, T. Kamikado, S. Yokoyama and T. Nagase, *Thin Solid Films*, 2008, **516**, 2762–2766.
53 A. Riposan and G.-y. Liu, *J. Phys. Chem. B*, 2006, **110**, 23926–23937.
54 T. Morita and S. M. Lindsay, *J. Am. Chem. Soc.*, 2007, **129**, 7262–7263.
55 J. Li, J. K. Tomfohr and O. F. Sankey, *Phys. Status Solidi B*, 2003, **239**, 80–87.
56 H. Basch and M. A. Ratner, *J. Chem. Phys.*, 2003, **119**, 11926–11942.
57 J. G. Kushmerick, *Mater. Today*, 2005, **July/Aug**, 26–30.
58 S. M. Lindsay, *Electrochem. Soc. Interface*, 2004, **Spring**, 26–30.
59 C. J. Xia, C. F. Fang, P. Zhao and H. C. Liu, *Eur. Phys. J. D*, 2010, **59**, 375–378.
60 K. B. Dhungana, S. Mandal and R. Pati, *J. Phys. Chem. C*, 2012, **116**, 17268–17273.
61 J. Zhou, G. Chen and B. Xu, *J. Phys. Chem. C*, 2010, **114**, 8587–8592.
62 J. Zhou, C. Guo and B. Xu, *J. Phys.: Condens. Matter*, 2012, **24**, 164029/1–164029/9.
63 J. Zhou and B. Xu, *Appl. Phys. Lett.*, 2011, **99**, 042104/1–042104/3.